Optimization of stabilized annealing of Al-Mg alloys utilizing machine learning algorithms

DOI:
10.1016/j.mtcomm.2023.106177

Document Version
Accepted author manuscript

Citation for published version (APA):
Xue, D., Wei, W., Shi, W., Zhou, X. R., Qi, J. T., Wen, S. P., Wu, X. L., Gao, K. Y., Xiong, X. Y., Huang, H., & Nie, Z. R. (2023). Optimization of stabilized annealing of Al-Mg alloys utilizing machine learning algorithms. *Materials Today Communications*, *35*, [106177]. https://doi.org/10.1016/j.mtcomm.2023.106177

Published in:
Materials Today Communications

Journal Pre-proof

Optimization of stabilized annealing of Al-Mg alloys utilizing machine learning algorithms

D. Xue, W. Wei, W. Shi, X.R. Zhou, J.T. Qi, S.P. Wen, X.L. Wu, K.Y. Gao, X.Y. Xiong, H. Huang, Z.R. Nie

PII: S2352-4928(23)00868-1

DOI: https://doi.org/10.1016/j.mtcomm.2023.106177

Reference: MTCOMM106177

To appear in: *Materials Today Communications*

Received date: 31 March 2023
Revised date: 26 April 2023
Accepted date: 9 May 2023

Please cite this article as: D. Xue, W. Wei, W. Shi, X.R. Zhou, J.T. Qi, S.P. Wen, X.L. Wu, K.Y. Gao, X.Y. Xiong, H. Huang and Z.R. Nie, Optimization of stabilized annealing of Al-Mg alloys utilizing machine learning algorithms, *Materials Today Communications,* (2023) doi:https://doi.org/10.1016/j.mtcomm.2023.106177

Optimization of stabilized annealing of Al-Mg alloys utilizing machine learning algorithms

D. Xue [a], W. Wei [a]*, W. Shi [b], X.R. Zhou [c], J.T. Qi [d], S.P. Wen [a], X.L. Wu [a], K.Y. Gao [a], X.Y. Xiong [a], H. Huang [a]**, Z.R. Nie [a]

[a] Key Laboratory of Advanced Functional Materials, Education Ministry of China, Beijing University of Technology, Beijing 100124, China

[b] Institute of Corrosion Science and Technology, Guangzhou 510530, China

[c] School of Materials, The University of Manchester, Manchester, M13 9PL, UK

Abstract

The corrosion properties of the alloy are influenced by the physical parameters involved in the preparation process. Experiments to explore the preparation process of Al-Mg alloys are very complex and time-consuming, and the amount of data is very limited. In this work, the analysis of the corrosion mechanism of Al-Mg alloy identified the alloy magnesium content, deformation, annealing temperature and time as important factors affecting the corrosion resistance of the alloy. Based on the existing experimental data, a machine learning framework that effectively promotes smart manufacturing is proposed. The results show that the machine learning framework constructed based on the existing experimental results can reliably predict the NAMLT values of the alloy. As more data is acquired, the method is expected to be used to adjust production processes for efficient and intelligent machining.

Key words: Al–Mg alloy; Machine learning; Microstructural; Corrosion; Annealing.

* Corresponding author, Address: Key Laboratory of Advanced Functional Materials, Education Ministry of China, Beijing University of Technology, Beijing 100124, China.
E-Mail address: weiwu@bjut.edu.cn (W. Wei)
** Corresponding author, Address: Key Laboratory of Advanced Functional Materials, Education Ministry of China, Beijing University of Technology, Beijing 100124, China.
E-Mail address: huanghui@bjut.edu.cn (H. Huang)

1. Introduction

Al-Mg alloys have been used as important structural materials in the shipbuilding and transportation industries, due to their high specific strength, excellent plastic toughness, corrosion resistance and weldability[1, 2]. The β phase (Al_3Mg_2) in Al-Mg alloy has high nucleation power, which can only be heterogeneously nucleated at the grain boundary and cannot be diffusely precipitated[3]. Therefore, the strength of Al-Mg alloy cannot be improved by heat treatment. The mechanical properties of Al-Mg alloy are mainly improved by solution strengthening of Mg and deformation strengthening. However, when Al-Mg alloys with Mg content above 3 wt.% are used for a prolonged period time at working temperature, the β phase will continue to precipitate at the grain boundaries, leading to the sensitivity of intergranular corrosion. [4, 5].

The solution to the problem of intergranular corrosion sensitivity is usually to stabilizing annealing[3, 6, 7]. Previous studies have shown that stabilized annealing causes intermittent precipitation of β phase at grain boundaries, which can block the extension of intergranular corrosion and thus enhance the corrosion resistance of the alloy[8, 9]. The temperature range for stabilization annealing is above 200°C, which is the temperature range for the recovery and recrystallization of the alloy. The deformation strengthening of the alloy will be reduced after stabilization annealing. At lower annealing temperatures, the alloy recovers and deformation strengthening can be partially retained. At higher annealing temperatures or longer times, the alloy recrystallizes and the deformation strengthening is completely lost. Therefore, an appropriate stabilization annealing process is the main factor affecting the properties of the alloy.

Experiments to explore the stabilization process of a single Al-Mg alloy are quite complex and time-consuming, and the amount of data is very limited. The stabilization annealing process of Al-Mg alloy depends on the Mg content of the alloy. Therefore, a model related to Mg content, stabilization annealing temperature and time is needed to predict the corrosion resistance of the alloy. Lim et al. developed a model related to the medium degree of sensitization, propagation direction and exposure time, which predicted the evolution of intergranular corrosion in AA5083. However, the construction of stabilized annealing models for alloys with different Mg contents has attracted little attention. Recently, artificial neural networks (ANN) have provided new methods for material modeling and process control[10,11]. ANN can self-identify patterns of input and output values without any prior natural hypothesis.

ANN does not require any knowledge of grain boundary precipitation and electrochemical corrosion. Therefore, ANN is applicable to simulate the corrosion resistance behavior of Al-Mg alloys under different stabilization annealing.

In this paper, the corrosion properties of Al-Mg alloys with different annealing processes were systematically studied. In addition, a model was developed to predict the corrosion properties with Mg content, deformation, stabilization annealing temperature and time as parameters.

2. Experimental and training data generation

The aluminum alloy ingot was subjected to homogenization heat treatment (475 ˚C/24 h) and then machined hot rolled to 20mm thickness. The hot rolled sheets are recrystallized annealed (350°C/2 h) and finally cold rolled with a controlled depression of 10%-25% in each pass, for a total deformation of 60% or 35%. The actual composition and deformation of the alloy are shown in Table 1.

Table 1 Sample processing details.

Sample	Mg content (wt%)	Deformation (%)
1#	3.9	60
2#	4.9	60
3#	6.1	60
4#	5.9	50
5#	6.0	35

2.1 Microstructure characterization

Microstructural characterization was performed by optical microscope, electron backscatter diffraction (EBSD) and transmission electron microscopy (TEM). The quantitative EBSD measurements were carried out on a Quanta 650 with a step size of 0.1 and the analysis software of channel 5 software. The EBSD samples were mechanically sanded and then electrolytically polished at 20 V for 15 s with an electrolyte of 5% perchloric acid and 95% methanol. The EBSD sample preparation was mechanically ground and then electropolished for 15 s at 20 V, with a temperature of 243 K, and an electrolyte of 5% perchloric acid and 95% methanol. The TEM samples were prepared by mechanical polishing to 70-100 μm, followed by shearing to 3 mm discs and finally by double-jet electropolishing at temperatures below -30°C, with the polishing of 30% nitric acid and 70% methanol. The TEM measurements were performed on the JEM-2100F at 200 kV.

2.2 Degree of sensitization

The corrosion resistance of Al-Mg alloy was tested by nitric acid mass loss test (NAMLT) under different stabilization annealing processes. Three parallel specimens of each state alloy were tested, according to the ASTM G67 standard. When the NAMLT value of the specimen is less than 15 mg/cm^2, the specimen is not sensitive to intergranular corrosion, indicating that the specimen has good resistance to intergranular corrosion. And when the NAMLT value is between 15-25 mg/cm^2, the type of corrosion occurring in the specimen may be uniform corrosion, pitting corrosion or intergranular corrosion, which requires further observation of the longitudinal section of the specimen. The NAMLT value is greater than 25 mg/cm^2, the specimen is in the intergranular corrosion-sensitive area, the specimen is more sensitive to intergranular corrosion.

3. Results and data analysis

3.1 Microstructure evolution

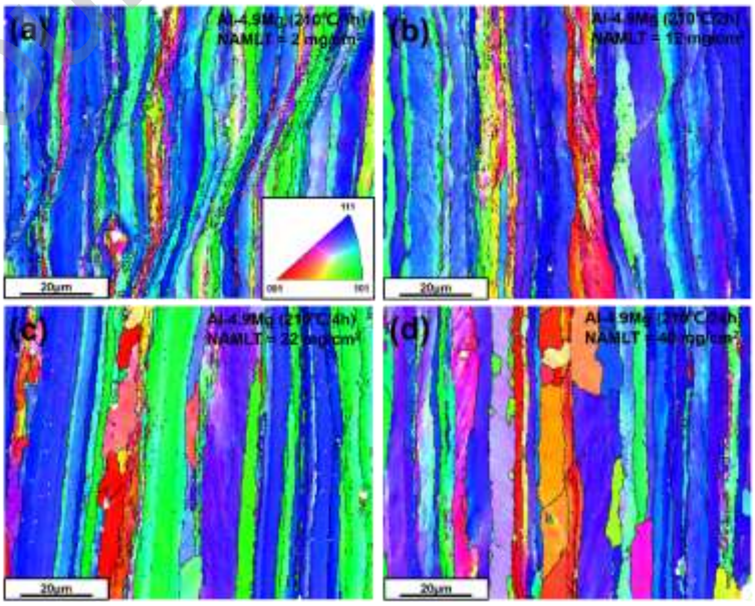

Fig. 1 Inverse pole figure maps of the 2# alloy (a) 210°C/1h annealing; (b) 210°C/2h annealing; (c) 210°C/4h annealing; (d) 210°C/24h annealing.

The microstructure of 2# alloy was characterized to explore the corrosion mechanism of the alloy. The inverse pole figure maps of the normal direction - rolling direction of 2 # alloy is shown in Fig. 1. The 2# alloy exhibits a typical deformed structure with elongated grains in the rolling direction, after annealing at 210°C for various times. A small amount of recrystallization is present in the alloy at 210°C/24h, which is difficult to occur due to the low annealing temperature (as shown in Fig. S1). The dislocation distribution of 2# alloy is shown in Fig. S2. It can be seen that the high-angle grain boundaries (HAGB) are distributed flat along the rolling direction. The low-angle grain boundary (LAGB) presents a network distribution, which decreases with the increase of annealing time.

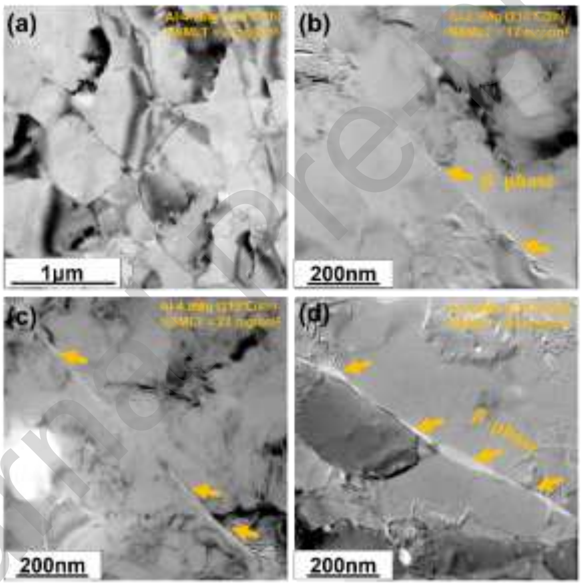

Fig. 2 TEM images showing the zone near grain boundary of the 2# alloy (a) 210℃/1h annealing; (b) 210℃/2h annealing; (c) 210℃/4h annealing; (d) 210℃/24h annealing.

After 210 ℃/2h annealing, the phase precipitates at the grain boundary, as shown in Fig. 2 (a). With the increase of annealing time, the coverage of the precipitates at the grain boundary increases, and the thickness of the precipitates becomes thicker, showing a continuous distribution. After annealing at 220°C for 24 hours, the maximum thickness of the β phase reached 53 nm with 81% coverage at the grain boundaries.

3.2 Corrosion resistance

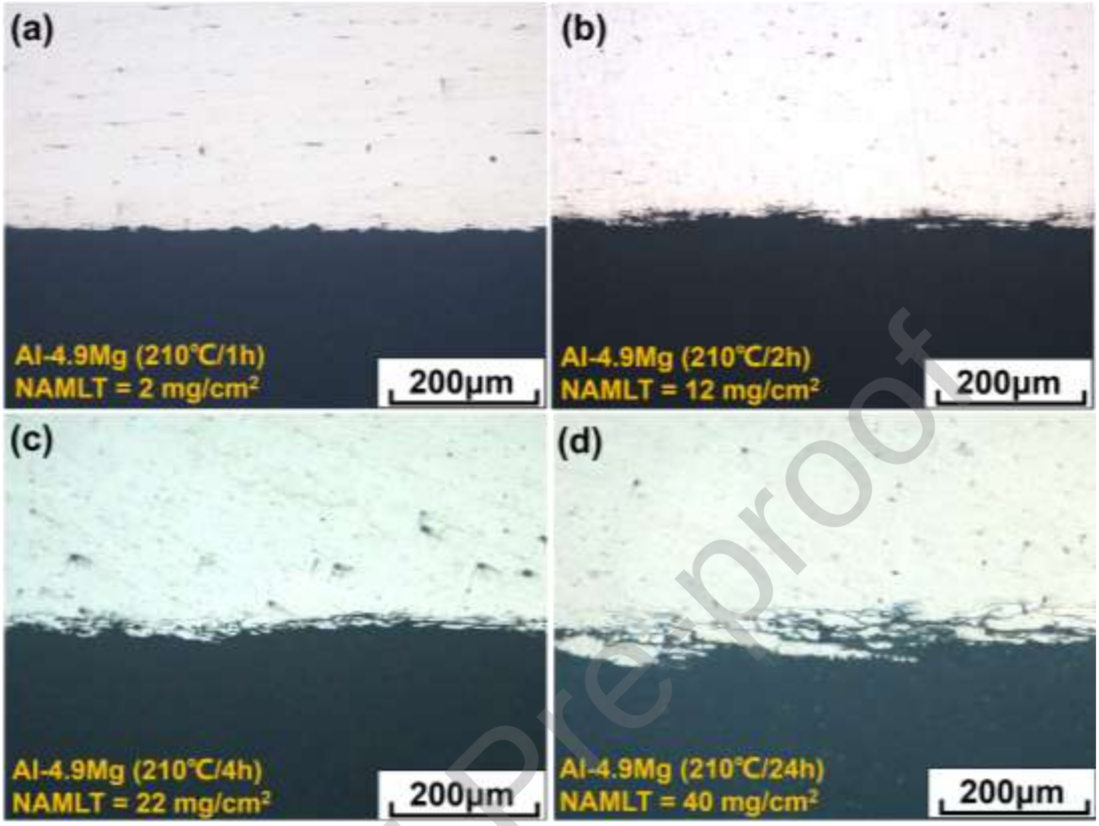

Fig. 3 Intergranular corrosion morphology: (a) 210°C/1h annealing; (b) 210°C/2h annealing; (c) 210°C/4h annealing; (d) 210°C/24h annealing.

The corrosion pattern is shown in Figure 3, where the white area is the matrix and the black is the area that has been corroded. The 2# alloy exhibited the best intergranular corrosion (IGC) resistance after 210°C/2h annealing with a NAMLT value of 2 mg/cm^2. The sample in Fig. 3(d) shows significant IGC penetration with a NAMLT of 40 mg/cm^2. The material can be considered as susceptible to IGC according to ASTM G67.

4. Discussion

4.1 Corrosion mechanism

The IGC results show that the alloy of 240/24h annealing exhibits poor corrosion resistance, which is attributed to the continuous precipitation of the β phase along the grain boundaries (see Fig.2). Xue et al[5]. have reported that β phase precipitates precipitate continuously along the HAGB providing a diffusion channel for intergranular corrosion, thereby reducing the corrosion resistance of the alloy. During annealing, due to the strong positive coupling between the Mg atoms and vacancies in the Al matrix with a binding energy of 0.2~0.4 eV, the Mg atoms tend to occupy vacancies at the grain boundaries, causing the Mg elements to segregate at the grain boundaries [12-14]. The annealing temperature was raised to obtain an intermittent β phase and the alloy showed excellent corrosion resistance, as shown in Fig. S3. Ding et al. reported that the β phase undergoes spheroidization, with intermittent distribution at grain boundaries, at the corresponding annealing temperatures [3]. The main nucleation sites of Al-Mg alloy grain boundary precipitates are along high angle grain boundaries, and no obvious phase precipitation is found at low angle grain boundaries [15, 16]. In cold deformed, the deformation bands are divided by flat large angle grain boundaries, providing nucleation sites for the precipitated phase and triggering continuous precipitation of the precipitated phase. In addition to the distribution of grain boundary precipitates, grain energy storage also plays an important role in corrosion propagation [17]. The distribution of grain boundary precipitates and grain energy storage are both affected by the stabilization annealing process. It can be concluded that the annealing process directly affects the corrosion resistance of Al-Mg alloys.

4.2 Data analysis

The ultimate goal of training a neural network is to ensure that the neural network model has good generalization ability to non-training samples. It is required that the model can effectively approximate the inherent laws contained in the sample, rather than considering the ability of the model to fit the training sample. Therefore, this paper adopts the K-fold cross-validation method to strengthen the generalization ability of the established network model. The training samples are evenly divided into 5 parts, 4 samples are selected in turn for training, and the remaining 1 part is used for verification. Backward propagation artificial neural network was used to construct a model to predict the corrosion resistance of the alloy. The schematic diagram of the artificial neural network is shown in Fig.4, which includes an input layer, an output layer and four hidden layers.

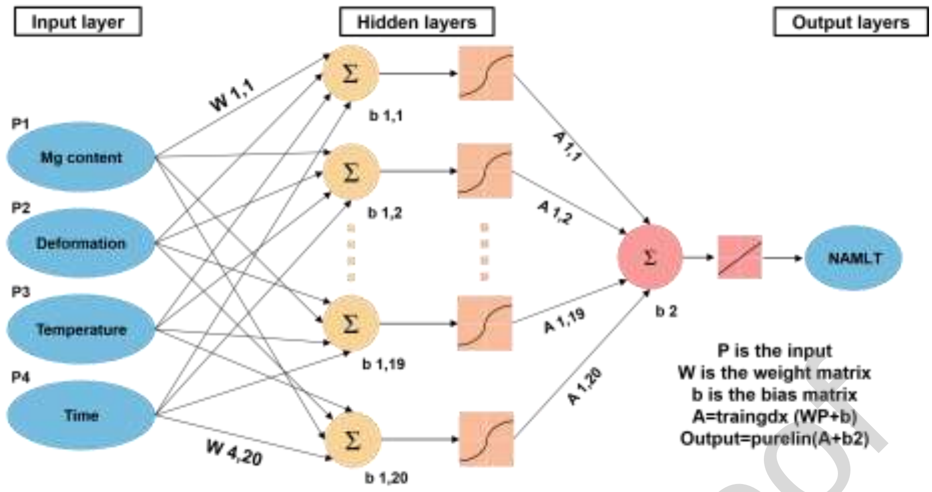

Fig. 4 Proposed machine learning algorithm.

In summary, the NAMLT of Al-Mg alloy is affected by factors such as Mg content and preparation process. Therefore, input layer includes Mg content, deformation, temperature and time, and the output layer is NAMLT. The sample data is normalized to improve the convergence reliability and speed of the model.

$$P' = 0.1 + 0.8\left(\frac{p - p_{min}}{p_{max} - p_{min}}\right) \tag{1}$$

Where, P is the original data and P' is the unified data corresponding to P. The corrosion properties of alloys in different states are listed in Table S1. Each hidden layer in the model has 20 nodes, the maximum number of iterations is 1000, and the target error is 0.000001.

4.2 Models verification

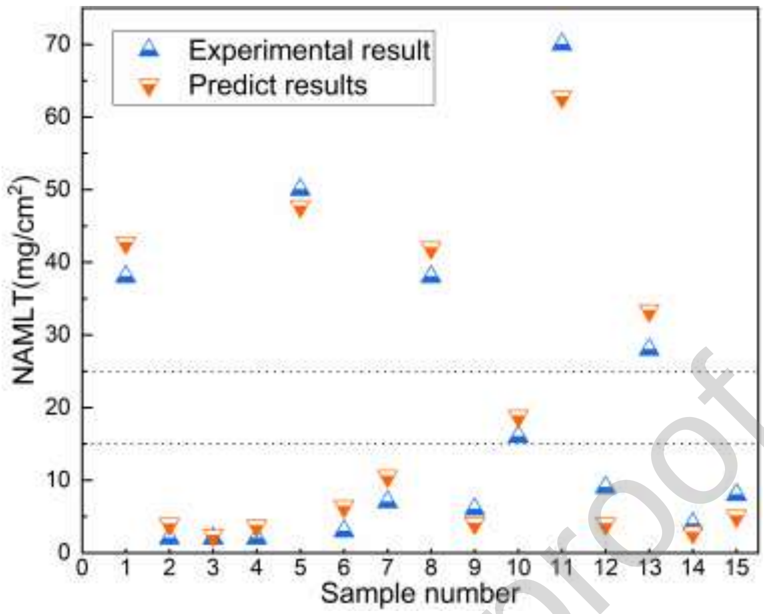

Fig. 5 Results of machine learning algorithms prediction.

The prediction results of the mechanical algorithm are shown in Fig. 5. It can be seen that the predicted results are in good agreement with the experimental results. Although there are individual large errors between the predicted results and the actual experimental results, such as sample 11, both results belong to the same level of corrosion according to the ASTM G67 standard. Therefore, the model can still accurately predict the corrosion results of Al-Mg alloys. To further investigate the accuracy of the predicted values, the mean absolute error between the experimental and predicted values was analyzed. The calculation formula is as follows:

$$MAE = \frac{1}{n}\sum_{i=1}^{n}|E_i - P_i| \tag{2}$$

Where MAE, P_i and E_i are the mean absolute error, predicted value and experimental value respectively. The MAE value of the model prediction is 0.195, indicating that the framework has a good prediction effect.

5. Conclusions

The analysis of the corrosion mechanism of Al-Mg alloy allows to identify the alloy magnesium content, deformation, annealing temperature and time as the key information affecting the corrosion resistance of alloy. Based on the correlation of composition-process-corrosion properties during the preparation of Al-Mg alloys, a machine learning framework to effectively promote intelligent manufacturing is proposed. The mechanical learning framework constructed from the available experimental results predicts results with an *MAE* of only 0.195, which implies that this model can reliably predict the NAMLT values of alloys.

Acknowledgements

This research was funded by National Key Research and Development Program of China (2021YFB3704202), General Program of Science and Technology Development Project of Beijing Municipal Education Commission (KM 202110005010), Innovative Research Group Project of the National Natural Science Fund (Grant No. 51621003).

Appendix A. Supplementary data

Supplementary data associated with this article can be found, in the online version.

References

[1] B.W. Yang, M.Q. Gao, Y. Wang, R.G. Guan, Dynamic recrystallization behavior and mechanical properties response of rheo-extruded Al–Mg alloys with various Mg contents, Mater Sci Eng A 849 (2022) 143450.

[2] Z.Z. Li, H.G. Yan, J.H. Chen, W.J. Xia, H.M. Zhu, B. X.Y. Su, Li, M. Song, Enhancing damping capacity and mechanical properties of Al-Mg alloy by high strain rate hot rolling and subsequent cold rolling, J Alloy Compd 908 (2022) 164677.

[3] Y.S. Ding, K.Y. Gao, H Huang, S.P. Wen, X.L. Wu, Z.R. Nie, S.S. Guo, R. Shao, C. Huang, D.J. Zhou, Nucleation and evolution of β phase and corresponding intergranular corrosion transition at 100–230 °C in 5083 alloy containing Er and Zr, Mater Design 174 (2019) 107778.

[4] M.L.C. Lim, R.G. Kelly, J.R. Scully, Overview of Intergranular Corrosion Mechanisms, Phenomenological Observations, and Modeling of AA5083, Corrosion 72 (2015) 198-220.

[5] D. Xue, W. Wei, W. Shi, Y.W. Guo, S.P. Wen, X.L. Wu, H. Huang, Z.R. Nie, Effect of cold

rolling on mechanical and corrosion properties of stabilized Al–Mg–Mn–Er–Zr alloy, J Mater Res Technol 15 (2021) 6329-6339.

[6] J.A. Lyndon, R.K. Gupta, M.A. Gibson, N. Birbilis, Electrochemical behaviour of the β-phase intermetallic (Mg2Al3) as a function of pH as relevant to corrosion of aluminium–magnesium alloys, Corros SCI 70 (2013) 290-293.

[7] M.L.C. Lim, R. Matthews, M. Oja, R. Tryon, R.G. Kelly, J.R. Scully, Model to predict intergranular corrosion propagation in three dimensions in AA5083-H131, Mater Design 96 (2016) 131-142.

[8] Y.C. Tzeng, C.H. Lin, Effects of stabilization treatment on the precipitation behavior of β phase and stress corrosion for AA5383-H15 alloys, J Mater Res 34 (2019) 1-9.

[9] Q.B. Ma, D. Zhang, L.Z. Zhuang, J.S. Zhang, Intergranular corrosion resistance of Zn modified 5××× series Al alloy during retrogression and re-aging treatment, Mater Charact 144 (2018) 264-273.

[10] S.R. Yousefi, O. Amiri, M. Salavati-Niasari. Control sonochemical parameter to prepare pure Zn0.35Fe2.65O4 nanostructures and study their photocatalytic activity, Ultrasonics Sonochemistry 59 (2019) 104619.

[11] S.R. Yousefi, A. Sobhani, M. Salavati-Niasari. A new nanocomposite superionic system (CdHgI4/HgI2): Synthesis, characterization and experimental investigation, Adv Powder Technol 28 (2017) 1258-1262.

[12] J.D. Embury, R.B. Nicholson, Dislocation sources in an aluminium alloy, Acta Metall 11 (1963) 347-354.

[13] M. Legros, G. Dehm, E. Arzt, T.J. Balk, Observation of giant diffusivity along dislocation cores, Science 319 (2008) 1646-9.

[14] Z.Q. Tang, F. Jiang, M.J. Long, J.Y. Jiang, H.F. Liu, M.M. Tong, Effect of annealing temperature on microstructure, mechanical properties and corrosion behavior of Al-Mg-Mn-Sc-Zr alloy, Appl Surf Sci 514 (2020) 146081.

[15] Y.F. Zhao, M.N. Polyakov, M. Mecklenburg, M.E. Kassner, A.M. Hodge,The role of grain boundary plane orientation in the β phase precipitation of an Al–Mg alloy, Scripta Mater 89 (2014) 49-52.

[16] W. Xu, T.C. Xin, B Zhang, X.L. Li, Stress corrosion cracking resistant nanostructured Al-Mg

alloy with low angle grain boundaries, Acta Mater 225 (2022) 117607.

[17] X. Zhang, X. Zhou, T. Hashimoto, J Lindsay, O. CillCa, C Luo, Z. Sun, X. Zhang, Z. Tang, The influence of grain structure on the corrosion behaviour of 2A97-T3 Al-Cu-Li alloy, Corros Sci 116 (2017) 14-21.

Credit Author Statement

D. Xue：Writing - Original Draft; Conceptualization; Investigation; Formal analysis.

W. Wei: Writing - Review & Editing; Conceptualization; Formal analysis; Methodology; Supervision.

W. Shi: Formal analysis.

X.R. Zhou: Formal analysis.

J.T. Qi: Formal analysis.

S.P. Wen: Formal analysis.

X.L. Wu: Software; Formal analysis.

K.Y. Gao: Formal analysis.

X.Y. Xiong: Formal analysis.

H. Huang: Software; Formal analysis; Supervision.

Z.R. Nie: Resources, Formal analysis.

Declaration of interests

☒ The authors declare that they have no known competing financial interests or personal relationships that could have appeared to influence the work reported in this paper.

☐The authors declare the following financial interests/personal relationships which may be considered as potential competing interests:

Graphical abstract